Efficient Wideband Source Localization Using Beamforming Invariance Technique

Ta-Sung Lee, *Member, IEEE*

***Abstract*— A novel scheme for wideband direction-of-arrival (DOA) estimation is proposed. The technique performs coherent signal subspace transformation by a set of judiciously constructed beamforming matrices. The beamformers are chosen to transform each of the narrowband array manifold vectors into the one corresponding to the reference frequency, regardless of the actual spatial distribution of the sources. The focused data correlation matrix can thus be obtained without any preliminary DOA estimation or iteration. A simplified version of the beamspace Root-MUSIC algorithm is developed and used in conjunction with the proposed method to efficiently localize multiple wideband sources with a linear, equally spaced array. Numerical simulations are conducted to demonstrate the efficacy of the new scheme.**

I. Introduction

THE problem of efficiently processing wideband array data for multiple sources localization has received considerable attention [1]–[11]. The idea of coherent signal subspace transformation was proposed by Wang and Kaveh [2] as an alternative to the classical incoherent signal subspace methods [1]. In the coherent signal subspace method (CSSM), the wideband array data are first decomposed into several narrowband components via FFT. Focusing matrices are then constructed to transform each of the narrowband DOA matrices into the one corresponding to the reference frequency bin. Application of eigen-based methods in conjunction with CSSM dictates that the DOA estimates be obtained with the effective focused data/noise correlation matrix pencil formed as the weighted average of the individual transformed narrowband correlation matrices. This is in contrast to the incoherent approach, in which individual processing of each narrowband array data component is performed, followed by a statistical combination of the resulting estimates from narrowband processing. Compared with the incoherent methods, CSSM has been shown to exhibit lower detection and resolution SNR threshold. The coherent method thus provides an efficient means of exploiting the full time-bandwith product of the wideband data.

Much work has been done along the lines of CSSM. Buckley and Griffiths [6] propose a broad-band signal-subspace spatial spectrum (BASS-ALE) estimator based on the eigenstructure of the broad-band spatial/temporal correlation matrix. In their approach, low-rank representation for wideband sources is used based on focusing operation, and lower source location bias is achieved by increasing the number of "location vectors." The tradeoff is an increase in computational load. An alternative to the BASS-ALE method is the steered covariance matrix (STCM) method described by Krolik and Swingler [9]. They consider the STCM as a slice through the correlation matrix taken at a primary steering direction. The STCM is computed for each direction of interest resulting in a greater computational complexity but, again, a smaller source location bias. A different approach developed by the same authors [11] is based on the concept of spatial resampling or interpolation. They exploit the characteristic structure of the array manifold vector, i.e., the components of the manifold vector depend on the source frequencies and the sensor element positions only through their product. Consequently, the same manifold vector may be obtained at different frequencies by suitably interpolating the narrowband array data components, that is, the manifold vector can be made invariant to the frequency. The resampling method is shown to exhibit good performance for a large angular region within the field-of-view (FOV) of the array. The major limitation is that their method is only applicable to linear, equally spaced (LES) arrays. Another class of CSSM-based wideband source localization schemes operating in beamspace were described by Buckley and Xu [5]. In their work, the wideband array data are first transformed into reduced dimension beamspace data via a beamforming matrix. CSSM is then applied to focus these beamspace data over the spatial passband of the beamformers. The advantage of working with CSSM in beamspace is the simplification in constructing the focusing matrices.

We here propose a beamspace wideband source localization scheme by exploiting the concept of beamspace manifold invariance. A design criterion based on the principle of least squares (LS) fit is employed to construct a beamforming matrix for each of the narrowband frequency bins extracted from the wideband array data. The beamforming matrices perform the same operation as do the focusing matrices described in [2], without knowing the spatial distribution of the wideband sources. One can regard the proposed method as beamspace CSSM, with the beamforming matrices judiciously chosen so that the resulting beamspace DOA matrices are essentially the same for all frequencies. The focused beamspace data/noise correlation matrix pencil can then be readily formed with the respective narrowband beamspace correlation matrices without any additional preliminary processing. The method provides a relatively wide range of effective operation in that perfect focusing can be achieved over a large angular region within

Manuscript received April 8, 1991; revised August 2, 1993. This work was supported by the National Science Council of R.O.C., under Grant NSC80-0404-E009-05. The associate editor coordinating the review of this paper and approving it for publication was S. Unnikrishna Pillai.

The author is with the Department of Communication Engineering, National Chiao Tung University, Hsinchu, Taiwan, Republic of China.

IEEE Log Number 9400392.

1053-587X/94$04.00

the FOV of the array as long as the normalized bandwidth of the wideband data is of moderate size.

For the special configuration of an LES array, we develop a computationally efficient implementation of the beamspace Root-MUSIC algorithm [12] via subarray beamforming and banded transformation. By subarray beamforming, the large-order Root-MUSIC signal polynomial is first reduced to one with the order equal to the beamspace dimension. The algorithm is further simplified by transforming the matrix representing the element space noise subspace into a banded form and converting the reduced-order signal polynomial into several polynomials with the order equal to the number of sources. These polynomials are then rooted in parallel to determine the DOA's. Aside from the saving in computations, the simplified algorithm avoids the vagueness of choosing a few desired signal roots from a large set of roots, as often occur in the execution of conventional Root-MUSIC.

The paper is organized as follows. In Section II, a brief review of wideband array signal modeling and the concept of CSSM is presented. In Section III, the beamforming-invariance focusing transformation is developed. Section IV demonstrates that the computational complexity associated with the beamspace Root-MUSIC algorithm can be greatly reduced via subarray beamforming and banded transformation. Finally, Section V presents simulation results confirming the efficacy of the proposed methods, and Section VI concludes the paper.

II. CSSM Model Formulation

We here consider the scenario of D wideband sources impinging on an array of M identical sensor elements. The sources are assumed to be in the far field of the array such that planewave assumption holds at each element. We further assume that the sensor elements have a common passband of width B_W centered at frequency f_c. Here, f_c and B_W are chosen according to the spectral content of the sources of interest. Additive wideband noise uncorrelated with the sources is present at each element with a known cross-spectral density matrix. The received waveform is first decomposed into J narrowband components via a bank of J bandpass filters, centered at f_j, $j = 1, \dots, J$, where $f_1 < f_2 < \cdots < f_J$, followed by the conventional I-Q demodulation and sampling to produce J sets of $M \times 1$ complex array data snapshot vectors

$$\mathbf{x}(n; f_j) = \mathbf{A}(f_j)\mathbf{s}(n; f_j) + \mathbf{v}(n; f_j) \qquad n = 1, \dots, N; j = 1, \dots, J \tag{1}$$

where the argument f_j denotes the dependence of the array data on different frequency bins. Note that the formation of narrowband components can also be done with suitable data segmentation and Fourier transform [2]. The ith component of the $D \times 1$ source vector $\mathbf{s}(n; f_j)$ represents the data received at some reference point of the array due to the ith source. The $M \times 1$ noise vector $\mathbf{v}(n; f_j)$ represents the noise present at the M elements. The ith column of the $M \times D$ DOA matrix $\mathbf{A}(f_j)$, accounting for the phase variation across the array due to the wavefront of the ith source, has the following structural form

$$\mathbf{a}(\vec{r}; f_j) = \left[e^{j2\pi f_j \frac{\vec{r}\cdot\vec{k}_1}{c}}, e^{j2\pi f_j \frac{\vec{r}\cdot\vec{k}_2}{c}}, \dots, e^{j2\pi f_j \frac{\vec{r}\cdot\vec{k}_M}{c}}\right]^T \tag{2}$$

with $\vec{r} = \vec{r}_i$, where

- $\vec{r}_i$ unit vector pointed at the ith source from the reference point
- $\vec{k}_m$ coordinate vector of the mth element with respect to the reference point
- c propagation speed of the source wave.

The vector $\mathbf{a}(\vec{r}; f_j)$ is here referred to as the narrowband manifold vector.

The core idea of CSSM is the construction of J focusing matrices $\mathbf{T}_j$, $j = 1, \dots, J$ such that the DOA matrices associated with different frequency bins can be transformed into the one corresponding to a preselected reference frequency f_o:

$$\mathbf{T}_j\mathbf{A}(f_j) = \mathbf{A}(f_o) \quad j = 1, \dots, J. \tag{3}$$

With the J focusing matrices applied to the respective data vectors, we obtain a set of new data vectors

$$\mathbf{T}_j\mathbf{x}(n; f_j) = \mathbf{A}(f_o)\mathbf{s}(n; f_j) + \mathbf{T}_j\mathbf{v}(n; f_j) \qquad n = 1, \dots, N; j = 1, \dots, J \tag{4}$$

having the identical DOA matrix structure. Application of correlation level DOA estimation methods in conjunction with CSSM dictates the formation of the "focused" data correlation matrix

$$\begin{aligned}\bar{\mathbf{R}}_{xx} &= \sum_{j=1}^{J} \alpha_j \mathbf{T}_j E\{\mathbf{x}(n; f_j)\mathbf{x}^H(n; f_j)\}\mathbf{T}_j^H \\ &= \mathbf{A}(f_o)\bar{\mathbf{R}}_{ss}\mathbf{A}^H(f_o) + \bar{\mathbf{R}}_{vv}\end{aligned} \tag{5}$$

where

$$\bar{\mathbf{R}}_{ss} = \sum_{j=1}^{J} \alpha_j E\{\mathbf{s}(n; f_j)\mathbf{s}^H(n; f_j)\} \tag{6}$$

$$\bar{\mathbf{R}}_{vv} = \sum_{j=1}^{J} \alpha_j \mathbf{T}_j E\{\mathbf{v}(n; f_j)\mathbf{v}^H(n; f_j)\}\mathbf{T}_j^H \tag{7}$$

and $\{\alpha_j\}$ is a set of preselected weights. The operation of CSSM in fact produces an effective narrowband data/noise correlation matrix pencil $\{\bar{\mathbf{R}}_{xx}, \bar{\mathbf{R}}_{vv}\}$ associated with f_o, with the effective source correlation matrix given by $\bar{\mathbf{R}}_{ss}$.

The benefits of using CSSM are twofold. First, by coherently combining the signal subspaces associated with different frequency bins, the effective source correlation matrix is essentially full rank, even in the extreme case of coherent sources. Second, the computational complexity is fairly low compared with the incoherent approach [2]. The only growth in computational load is the formation of J focusing matrices and the focused correlation matrix pencil. In spite of these beneficial aspects, CSSM requires a set of preliminary DOA estimates in order to construct the focusing matrices. As a consequence, large estimation bias occurs when the focusing matrices are in error [9]. An iterative procedure is suggested

[2] to improve the accuracy of the DOA estimates at the cost of higher computational complexity. As a remedy, the directional derivative constrained (DDC) method [7] was proposed as a means of expanding the effective angular range of focusing at the cost of poorer performance. Research efforts have been made on the development of perfect focusing, i.e., focusing without preliminary DOA estimates and iterations [4], [8], [11]. In this paper, we propose a new method of perfect focusing based on the concept of beamforming-invariance (BI) transformation.

III. Beamforming- Invariance Transformation

We here develop a beamforming technique that can achieve nearly perfect focusing over a specified angular region within the FOV of the array. The idea is to conduct beamspace transformation [5] at each of the J frequency bins, with the beamforming matrices judiciously chosen so that the corresponding beam patterns are essentially identical for all frequencies. For simplicity, consider first the patterns associated with a single beam:

$$w(\vec{r}; f_j) = \mathbf{w}_j^H \mathbf{a}(\vec{r}; f_j) \quad j = 1, \ldots, J \tag{8}$$

where $\mathbf{w}_j$ is the $M \times 1$ complex weight vector employed at f_j. Due to the discrete nature of the array, it is in general not possible to find two weight vectors that produce completely identical beam patterns at two different frequencies, except for the trivial case of zero weighting. As an approximation method, we propose a LS fit procedure for constructing weight vectors that nearly produce frequency-invariant beam patterns.

A convenient measure of the proximity between the two patterns $w(\vec{r}; f_i)$ and $w(\vec{r}; f_j)$ is the generalized L_2 distance

$$\begin{aligned} d_{ij} &= \int_\Omega \rho(\vec{r}) |w(\vec{r}; f_i) - w(\vec{r}; f_j)|^2 d\vec{r} \\ &= \int_\Omega \rho(\vec{r}) |\mathbf{w}_i^H \mathbf{a}(\vec{r}; f_i) - \mathbf{w}_j^H \mathbf{a}(\vec{r}; f_j)|^2 d\vec{r} \end{aligned} \tag{9}$$

where Ω is a sector of the unit sphere representing the FOV of the array. The weighting function $\rho(\vec{r})$ is incorporated to enhance the approximation within a preselected angular region. The weight vectors possessing "beamforming-invariance" are determined in accordance with the minimum-distance criterion

$$\min_{\mathbf{w}_i, \mathbf{w}_j} \int_\Omega \rho(\vec{r}) |\mathbf{w}_i^H \mathbf{a}(\vec{r}; f_i) - \mathbf{w}_j^H \mathbf{a}(\vec{r}; f_j)|^2 d\vec{r} \quad \textit{subject to}: \quad \mathbf{w}_i \neq \mathbf{0} \neq \mathbf{w}_j \tag{10}$$

where the constraint is imposed to assure nontrivial solutions. A major consideration in beamforming is that the beam pattern should exhibit good physical properties such as high SNR gain and low sidelobes. To incorporate these into the BI beamformer, we propose that a desired weight vector $\mathbf{w}_o$ associated with a preselected reference frequency f_o within the passband of the array is chosen first. The BI weight vectors associated with the J frequencies are then determined by

$$\min_{\mathbf{w}_j} \int_\Omega \rho(\vec{r}) |\mathbf{w}_o^H \mathbf{a}(\vec{r}; f_o) - \mathbf{w}_j^H \mathbf{a}(\vec{r}; f_j)|^2 d\vec{r} \quad j = 1, \ldots, J. \tag{11}$$

Note that f_o need not be one of $f_j, j = 1, \ldots, J$. The solutions to (11) are given by

$$\mathbf{w}_j = \mathbf{U}_j^{-1} \mathbf{S}_j \mathbf{w}_o \quad j = 1, \ldots, J \tag{12}$$

where

$$\mathbf{U}_j = \int_\Omega \rho(\vec{r}) \mathbf{a}(\vec{r}; f_j) \mathbf{a}^H(\vec{r}; f_j) d\vec{r} \quad j = 1, \ldots, J \tag{13}$$

$$\mathbf{S}_j = \int_\Omega \rho(\vec{r}) \mathbf{a}(\vec{r}; f_j) \mathbf{a}^H(\vec{r}; f_o) d\vec{r} \quad j = 1, \ldots, J. \tag{14}$$

It is noteworthy that $\mathbf{U}_j$ may be ill conditioned if the FOV is too small. However, we do not here concern ourselves with the problem of small FOV. The reason is that if the FOV is rather small, then much information is available for the choosing of the preliminary DOA estimates. In this case, the regular version of CSSM would be the appropriate method of focusing.

A physical interpretation of the BI method is as follows. If a wideband source moves across the FOV of the array, then a set of essentially identical output waveforms (except possibly for a complex scalar multiple) can be observed at the J beamformer outputs. One can thus regard the BI method as a means of compressing the high-dimension element space wideband data into the low-dimension beamspace narrowband data associated with f_o.

A. Beamspace Focusing with BI Transformation

In beamspace eigen-based methods, multiple beams are formed over the spatial band of interest to achieve effective reception of the source signals. This may be accomplished by using a set of K beamforming weight vectors $\mathbf{w}_{jk}$, $k = 1, \ldots, K$ to simultaneously form K linear combinations of the array data at f_j. Mathematically speaking, the $M \times 1$ element space data snapshot vectors are converted into $K \times 1$ beamspace data snapshot vectors via

$$\mathbf{x}_B(n; f_j) = \mathbf{W}_j^H \mathbf{x}(n; f_j) \quad n = 1, \ldots, N; j = 1, \ldots, J \tag{15}$$

where $\mathbf{W}_j$, $j = 1, \ldots, J$ are the respective $M \times K$ beamforming matrices employed at the J frequencies

$$\mathbf{W}_j = [\mathbf{w}_{j1} | \mathbf{w}_{j2} | \cdots | \mathbf{w}_{jK}] \; j = 1, \ldots, J \tag{16}$$

Here, K is chosen to be such that $D < K \leq M$. The beamspace data snapshot vectors have the same structural form as the original array snapshot vectors

$$\mathbf{x}_B(n; f_j) = \mathbf{B}(f_j) \mathbf{s}(n; f_j) + \mathbf{v}_B(n; f_j) \quad n = 1, \ldots, N; j = 1, \ldots, J \tag{17}$$

where

$$\mathbf{B}(f_j) = \mathbf{W}_j^H \mathbf{A}(f_j) \; j = 1, \ldots, J \tag{18}$$

and

$$\mathbf{v}_B(n; f_j) = \mathbf{W}_j^H \mathbf{v}(n; f_j) \quad n = 1, \ldots, N; j = 1, \ldots, J \tag{19}$$

are the beamspace DOA matrices and noise vectors, respectively. The concept of BI prompts us to choose $\mathbf{W}_j$, $j = 1, \ldots, J$ in accordance with the procedure outlined in (11)–(14). In this case, we first determine a set of K reference weight vectors $\mathbf{w}_{ok}$, $k = 1, \ldots, K$, associated with f_o. We then construct the K weight vectors associated with the J frequencies as follows:

$$\mathbf{w}_{jk} = \mathbf{U}_j^{-1}\mathbf{S}_j\mathbf{w}_{ok} \quad k = 1, \ldots, K; j = 1, \ldots, J. \tag{20}$$

Putting in matrix form, we get

$$\mathbf{W}_j = \mathbf{U}_j^{-1}\mathbf{S}_j\mathbf{W}_o \quad j = 1, \ldots, J \tag{21}$$

where

$$\mathbf{W}_o = [\mathbf{w}_{o1}|\mathbf{w}_{o2}|\cdots|\mathbf{w}_{oK}] \tag{22}$$

is the reference beamforming matrix. Due to the BI property, we have $\mathbf{B}(f_j) \approx \mathbf{B}(f_o)$, $j = 1, \ldots, J$, such that the beamspace data snapshot vectors in (17) are fully characterized by a single beamspace DOA matrix $\mathbf{B}(f_o)$ representing the beamspace signal subspace associated with f_o. CSSM may then be applied to obtain a focused beamspace data correlation matrix

$$\bar{\mathbf{Q}}_{xx} = \sum_{j=1}^{J} \alpha_j E\{\mathbf{x}_B(n; f_j)\mathbf{x}_B^H(n; f_j)\} \approx \mathbf{B}(f_o)\bar{\mathbf{R}}_{ss}\mathbf{B}^H(f_o) + \bar{\mathbf{Q}}_{vv} \tag{23}$$

where $\bar{\mathbf{R}}_{ss}$ is as defined in (6), and

$$\bar{\mathbf{Q}}_{vv} = \sum_{j=1}^{J} \alpha_j E\{\mathbf{v}_B(n; f_j)\mathbf{v}_B^H(n; f_j)\}. \tag{24}$$

The operation of BI-CSSM produces an effective narrowband beamspace data/noise correlation matrix pencil $\{\bar{\mathbf{Q}}_{xx}, \bar{\mathbf{Q}}_{vv}\}$ associated with f_o with, again, the effective source correlation matrix given by $\bar{\mathbf{R}}_{ss}$.

B. Design of Reference Beamforming Matrix

Several criteria have been proposed for the design of "optimum" beamforming matrices for narrowband applications. Lee and Wengrovitz [13] derived the beamforming matrix that minimizes the resolution threshold for two closely spaced sources. Anderson [14] derived the beamforming matrix which retains the full dimension element space Cramér-Rao lower bound (CRLB) in beamspace. As an alternative, Forster and Vezzosi [15] proposed the idea of constructing beamformers using the prolate spheroidal sequences. Their method leads to the optimum beamforming matrix in that the total SNR gain associated with the K beamformers is maximized over the specified spatial band. It should be pointed out that the above results were obtained based on some idealized assumptions such as uncorrelated sources or spatially white Gaussian noise. For a more practical consideration, it is preferable to employ beamformers exhibiting high SNR gain within the desired spatial band and yet uniformly low sidelobes in order to suppress unwanted out-of-band interfering sources. A well-known example exhibiting uniformly low sidelobes for LES arrays is the Chebyshev beamformer. It is conceivable that in order to retain the merits of the optimum beamformers, when used in conjunction with BI-CSSM, one must assure that beamspace focusing be performed successfully. To this end, we propose a method of constructing the reference beamforming matrix that exhibits both optimality and small focusing error.

Our goal here is to determine an orthonormal basis for the subspace of "minimum focusing error." Let $\mathbf{E}_W$ be an $M \times K'$ matrix satisfying $\mathbf{E}_W^H\mathbf{E}_W = \mathbf{I}$, where $K \leq K' \leq M$. If we use $\mathbf{E}_W$ as the reference beamforming matrix, then, from (21), the resulting total focusing error is given by

$$E_f = \frac{1}{J}\sum_{j=1}^{J}\int_{\Omega} \rho(\vec{r})||\mathbf{E}_W^H\mathbf{a}(\vec{r}; f_o) - \mathbf{E}_W^H\mathbf{S}_j^H\mathbf{U}_j^{-1}\mathbf{a}(\vec{r}; f_j)||^2 d\vec{r} = tr\{\mathbf{E}_W^H\mathbf{S}_U\mathbf{E}_W\} \tag{25}$$

where $||\cdot||$ denotes the vector 2-norm, $tr\{\cdot\}$ denotes the trace, and

$$\mathbf{S}_U = \frac{1}{J}\sum_{j=1}^{J}(\mathbf{S}_o - \mathbf{S}_j^H\mathbf{U}_j^{-1}\mathbf{S}_j) \tag{26}$$

where $\mathbf{S}_o$ is given by (14) with f_j replaced by f_o. The optimum $\mathbf{E}_W$ that minimizes E_f is composed of the K' eigenvectors (EV) of $\mathbf{S}_U$ associated with the K' smallest eigenvalues (ev), which are denoted as λ_k, $k = 1, \ldots, K'$. Moreover, the minimum value of E_f equals $E_{\min} = \sum_{k=1}^{K'}\lambda_k$. We may thus regard these EV's as the orthonormal basis vectors spanning the K'-dimensional subspace of minimum focusing error and use them as the basis for constructing the reference beamforming matrix. Suppose that a desired beamforming matrix

$$\mathbf{W}_d = [\mathbf{w}_{d1}|\mathbf{w}_{d2}|\cdots|\mathbf{w}_{dK}] \tag{27}$$

is selected. We wish to determine a set of reference weight vectors as linear combinations of the columns of $\mathbf{E}_W$, which approximate the desired weight vectors in LS sense. Putting in matrix form, we have

$$\min_{\mathbf{W}_o = \mathbf{E}_W\mathbf{\Psi}} ||\mathbf{W}_o - \mathbf{W}_d||_F^2 \tag{28}$$

where $\mathbf{\Psi}$ is a $K' \times K$ linear combination coefficient matrix, and $||\cdot||_F$ denotes the Frobenius norm. The optimum $\mathbf{W}_o$ is given by

$$\mathbf{W}_o = \mathbf{E}_W(\mathbf{E}_W^H\mathbf{E}_W)^{-1}\mathbf{E}_W^H\mathbf{W}_d. \tag{29}$$

Geometrically speaking, we have projected the columns of $\mathbf{W}_d$ onto the subspace of minimum focusing error.

The general relationship between the normalized bandwidth $\bar{B}_W = B_W/f_c$ and the focusing error is easily derived. For small $\bar{B}_W$, the corresponding focusing error is undoubtedly small. As $\bar{B}_W$ is increased (and so is J), we note that the disparity between $\mathbf{S}_o$ and $\mathbf{S}_j^H\mathbf{U}_j^{-1}\mathbf{S}_j$, $j = 1, \ldots, J$, becomes significant. Due to the averaging effect in (26), $\mathbf{S}_U$ will approach a relatively high rank matrix, leading to a relatively large $E_{\min}$. This implies that the focusing error associated with the reference beamforming matrix constructed according to (29) is also large. Since most desired beamforming matrices can be approximated by $\mathbf{E}_W$ to a certain extent, we arrive at the conjecture that the focusing error is indeed an increasing function of $\bar{B}_W$. It is therefore conceivable that working with a large $\bar{B}_W$ in BI-CSSM does not necessarily improve the estimation performance as the effect of increase in time-bandwidth product is likely to be offset by the extra focusing error incurred.

C. Design Examples

The following experiments were conducted to access the efficacy of the BI transformation. For a simple demonstration, we assume that an LES array was employed. The general form of the manifold vector associated with an LES array consisting of M identical elements and operating with frequency f is given by

$$\mathbf{a}(u; f) = \left[1, e^{j\tau f u}, e^{j2\tau f u}, \ldots, e^{j(M-1)\tau f u}\right]^T \tag{30}$$

with $\tau = 2\pi d/c$, where d is the spacing between two adjacent elements. The sine-space angle u is defined as $u = \sin(\theta)$, where θ is the angle measured with respect to the broadside of the array. Note that we have set the reference point of the array to be at its first element. For the experiment, we choose $M = 15$, $\bar{B}_W = 40\%$, and $f_c = c/2d$, i.e., the elements are equally spaced by a half wavelength corresponding to f_c.

For the execution of the BI transformation, the frequency band was decomposed into $J = 33$ uniformly distributed subbands. The reference beamforming matrix $\mathbf{W}_o$ was constructed at $f_o = f_1$ in accordance with the procedure outlined in (27)–(29), with $K' = 9$ and $\mathbf{W}_d$ composed of weight vectors associated with $K = 7$ Chebyshev beams with -30 dB sidelobes pointed at $\theta = 0°, \pm 7.7°, \pm 15.5°$, and $\pm 23.6°$. The Chebyshev beamformer is optimum in that given a specified sidelobe level, the corresponding mainlobe width is minimized. Fig. 1 shows the superposition of the beam patterns associated with $\mathbf{W}_o$. We see that low sidelobes were retained by $\mathbf{W}_o$. Note that we chose $f_o = f_1$ in order to alleviate the grating lobe problem. In the construction of the remaining 32 beamforming matrices via (21), the FOV was set to be $\Omega = [-1.0, 1.0]$ in u domain. The weighting function $\rho(u)$ was chosen as

$$\begin{aligned} \rho(u) &= 1.0 \qquad |u| \le 0.7 \\ &= 0.5 \qquad 0.7 < |u| \le 1 \end{aligned} \tag{31}$$

to enhance the focusing effect within the sector $[-44°, 44°]$.

To evaluate the quality of focusing numerically, we calculated the normalized focusing error spectrum

$$\bar{E}_f(u) = \left(\frac{\sum_{j=1}^{J} ||\mathbf{W}_o^H \mathbf{a}(u; f_o) - \mathbf{W}_j^H \mathbf{a}(u; f_j)||^2}{||\mathbf{W}_o^H \mathbf{a}(u; f_o)||^2} \right)^{1/2} \tag{32}$$

and plotted the result in Fig. 2. The flat valley over $[-44, 44°]$ confirms our previous statement. The relatively large focusing error occurring near the endfires was mainly caused by the grating lobes associated with the high frequencies. Since the angular separation between the mainlobe and the nearest grating lobes is approximately $c/f_j d$ (in u-domain) for the jth band, it is conceivable that effective focusing can only be achieved within a sector of width $c/f_J d$. For the above example, $f_J \approx 1.2 f_c$ such that the size of the sector of effective focusing is approximately 1.67.

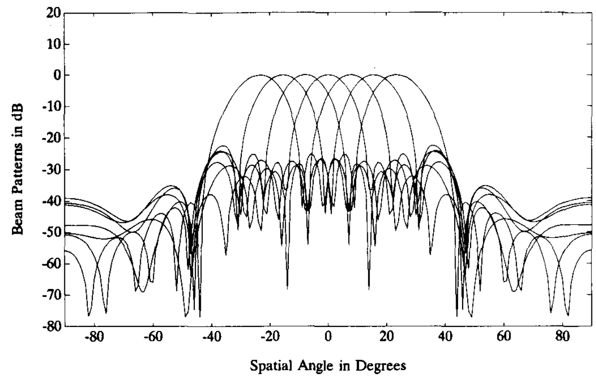

Fig. 1. Superposition of $K = 7$ minimum focusing error beam patterns generated by an $M = 15$ element LES array.

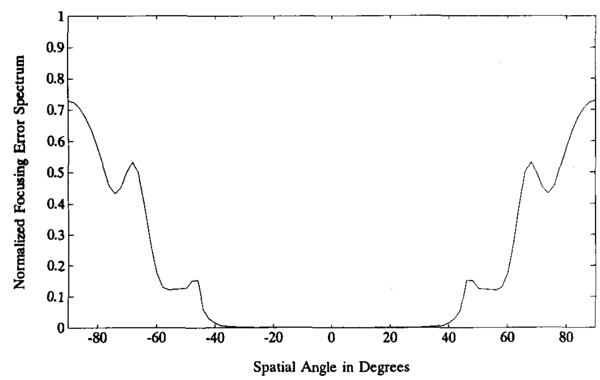

Fig. 2. Normalized focusing error spectrum associated with $J = 33$ sets of focused beam patterns generated by an $M = 15$ element LES array with enhanced focusing within $[-44, 44°]$.

IV. BI-CSSM/Root-Form Eigen-Based DOA Estimation

For simplicity, we will consider only the operation associated with f_o and omit the argument of frequency in the relevant terms. Application of beamspace eigen-based methods on the BI-CSSM focused data dictates that the source DOA's be determined via the null spectrum

$$\Phi(\vec{r}) = \mathbf{a}^H(\vec{r}) \mathbf{W}_o \bar{\mathbf{E}}_B \mathbf{P} \bar{\mathbf{E}}_B^H \mathbf{W}_o^H \mathbf{a}(\vec{r}) \tag{33}$$

where $\bar{\mathbf{E}}_B$, which is referred to as the beamspace noise EV matrix, is the $K \times (K-D)$ matrix composed of the generalized eigenvectors of $\{\hat{\mathbf{Q}}_{xx}, \bar{\mathbf{Q}}_{vv}\}$ associated with the $K-D$ smallest generalized eigenvalues, where $\hat{\mathbf{Q}}_{xx}$ is an estimate of $\bar{\mathbf{Q}}_{xx}$. $\mathbf{P}$ is a positive-semidefinite matrix serving to weight the respective columns of $\bar{\mathbf{E}}_B$. As two well-known examples, beamspace MUSIC corresponds to $\mathbf{P} = \mathbf{I}$ and beamspace Minimum-Norm [16] corresponds to $\mathbf{P} = \mathbf{c}\mathbf{c}^H$, where $\mathbf{c}$ is the transpose of the first row of $\mathbf{W}_o\bar{\mathbf{E}}_B$.

For LES arrays, the null spectrum in (33) can be converted into the $2(M-1)$th order "signal polynomial" [12]

$$\Phi(z) = \mathbf{a}^T(z^{-1})\mathbf{W}_o\bar{\mathbf{E}}_B\mathbf{P}\bar{\mathbf{E}}_B^H\mathbf{W}_o^H\mathbf{a}(z) \tag{34}$$

where

$$\mathbf{a}(z) = \left[1, z, \ldots, z^{M-1}\right]^T \tag{35}$$

with $z = e^{j\tau f_o u}$. With a set of D "signal roots" $\hat{z}_i$, $i = 1, \ldots, D$ extracted from $\Phi(z)$, the DOA's can be determined by $\hat{u}_i = \arg\{\hat{z}_i\}/\tau f_o$, $i = 1, \ldots, D$. Note that the coefficients of $\Phi(z)$ exhibit conjugate symmetry such that the corresponding $2(M-1)$ roots form $M-1$ conjugate reciprocal pairs. As a consequence, only $M-1$ distinct values are observed regarding the phase angles of the $2(M-1)$ roots. Rao and Hari [17] show that "root-form" methods exhibit a higher resolution capability than their "spectral-form" counterparts in dealing with closely-spaced sources. They argue that a zero of the null spectrum having a large radial error will cause the corresponding spectral minima to be less defined but does not affect the DOA estimates. In addition, it is found that root-form methods are more robust to certain modeling errors [18].

In spite of the merits stated above, working with root-form methods may be computationally expensive due to the need of large order polynomial rooting. To remedy this, we propose in this section a scheme that can avoid the rooting of a large-order signal polynomial while retaining the resolution capability of root-form methods. The new algorithm involves three stages. First, the signal polynomial is reduced from order $2(M-1)$ to $2(K-1)$ via judiciously performed subarray beamforming. Second, the reduced-order signal polynomial is converted into several $2D$th (or Dth) order polynomials via a banded transformation of the corresponding reduced noise EV matrix. Third, signal roots are extracted by rooting these polynomials in parallel.

A. Polynomial-Order Reduction via Subarray Beamforming

Consider an M-element LES array as consisting of $L = M-K+1$ overlapping K-element LES subarrays, as depicted in Fig. 3. We refer to these identical subarrays as A_K. Define the $K \times M$ selection matrices that select from the full array data snapshot vectors the respective subarray data snapshot vectors

$$\mathbf{\Gamma}_l\mathbf{x}(n) = \mathbf{x}_K^{(l)}(n) \quad n = 1, \ldots, N; l = 1, \ldots, L \tag{36}$$

where $\mathbf{x}_K^{(l)}(n)$ denotes the $K \times 1$ data snapshot vectors received at the lth subarray. It is easily seen from Fig. 3 that $\mathbf{\Gamma}_l$ is given by

$$\mathbf{\Gamma}_l = \left[\mathbf{O}_{K\times(l-1)}|\mathbf{I}_{K\times K}|\mathbf{O}_{K\times(M-K-l+1)}\right] l = 1, \ldots, L \tag{37}$$

with the subscripts indicating the sizes of the respective identity and zero matrices. Assume that the same $K \times 1$ weight vector $\mathbf{g} = [g_1, g_2, \ldots, g_K]^T$ is applied at each of the subarrays, producing a set of $L \times 1$ vectors

$$\mathbf{x}_L(n) = \begin{bmatrix} \mathbf{g}^H\mathbf{x}_K^{(1)}(n) \\ \mathbf{g}^H\mathbf{x}_K^{(2)}(n) \\ \vdots \\ \mathbf{g}^H\mathbf{x}_K^{(L)}(n) \end{bmatrix} = \mathbf{G}^H\mathbf{x}(n) \qquad n = 1, \ldots, N \tag{38}$$

representing the data snapshots received at the L subarray beamformer outputs, where

$$\mathbf{G} = \left[\mathbf{\Gamma}_1^T\mathbf{g}|\mathbf{\Gamma}_2^T\mathbf{g}|\cdots|\mathbf{\Gamma}_L^T\mathbf{g}\right] = \begin{bmatrix} g_1 & & & 0 \\ \vdots & \ddots & & \\ & & \ddots & g_1 \\ g_K & & & \vdots \\ & \ddots & & \\ & & \ddots & \\ 0 & & & g_K \end{bmatrix}. \tag{39}$$

We can now regard $\mathbf{x}_L(n)$, $n = 1, \ldots, N$ as the data snapshot vectors obtained from a L-element LES array, which is denoted as A_L, and apply a $L \times 1$ weight vector $\mathbf{c}$ to form

$$x_B(n) = \mathbf{c}^H\mathbf{x}_L(n) = (\mathbf{G}\mathbf{c})^H\mathbf{x}(n) = \mathbf{w}^H\mathbf{x}(n) \qquad n = 1, \ldots, N. \tag{40}$$

It is readily seen that $\mathbf{w} = \mathbf{G}\mathbf{c}$ is the effective weight vector acting on the entire array. In contrast to (40), we may consider the beamforming to be performed first on A_L, treating the L subarrays as "super elements." With such an array configuration, we may apply an $L \times 1$ weight vector $\mathbf{c} = [c_1, c_2, \ldots, c_L]^T$ to produce a set of $K \times 1$ "vector data snapshots"

$$\mathbf{x}_K(n) = \sum_{l=1}^{L} c_l^*\mathbf{x}_K^{(l)}(n) = \mathbf{C}^H\mathbf{x}(n) \qquad n = 1, \ldots, N \tag{41}$$

where

$$\mathbf{C} = \sum_{l=1}^{L} c_l\mathbf{\Gamma}_l^T = \begin{bmatrix} c_1 & & & 0 \\ \vdots & \ddots & & \\ & & \ddots & c_1 \\ c_L & & & \vdots \\ & \ddots & & \\ & & \ddots & \\ 0 & & & c_L \end{bmatrix}. \tag{42}$$

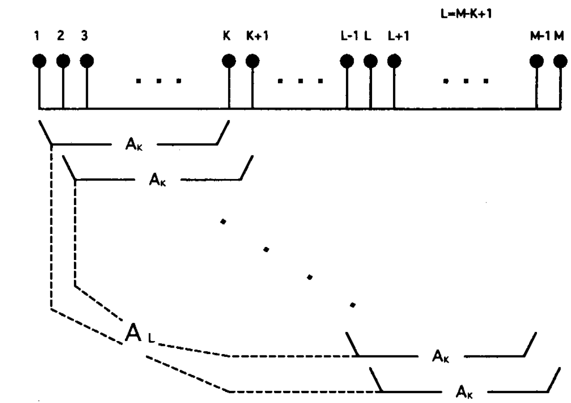

Fig. 3. Subarray structure associated with an LES array.

These vector data snapshots can be regarded as "data snapshot vectors" obtained from A_K. In this case, applying a $K\times 1$ weight vector $\mathbf{g}$ forms

$$x_B(n) = \mathbf{g}^H\mathbf{x}_K(n) = (\mathbf{C}\mathbf{g})^H\mathbf{x}(n) = \mathbf{w}^H\mathbf{x}(n) \quad n = 1,\ldots,N. \tag{43}$$

We conclude from (40) and (43) that the full weight vector exhibits two types of decomposition:

$$\mathbf{w} = \mathbf{G}\mathbf{c} = \mathbf{C}\mathbf{g} \tag{44}$$

Invoking the banded, Toeplitz structure of $\mathbf{C}$ or $\mathbf{G}$, we have

$$\mathbf{w}^H\mathbf{a}(z) = \{\mathbf{g}^H\mathbf{a}_K(z)\}\{\mathbf{c}^H\mathbf{a}_L(z)\} \tag{45}$$

where $\mathbf{a}_K(z)$ and $\mathbf{a}_L(z)$ are given by (35) with M replaced by K and L, respectively. Similarly, we can get

$$\mathbf{a}^T(z^{-1})\mathbf{w} = \{\mathbf{a}_K^T(z^{-1})\mathbf{g}\}\{\mathbf{a}_L^T(z^{-1})\mathbf{c}\}. \tag{46}$$

We now develop a beamspace transformation scheme based on the concept of weight vector decomposition. The idea is to construct K reference weight vectors with the following forms:

$$\mathbf{w}_{ok} = \mathbf{G}_k\mathbf{c} = \mathbf{C}\mathbf{g}_k \quad k = 1,\ldots,K \tag{47}$$

where $\mathbf{G}_k$ is given by (39) with $\mathbf{g}$ replaced by $\mathbf{g}_k$. The key point is that $\mathbf{w}_{ok}$, $k = 1,\ldots,K$, contain the same "weight factor" $\mathbf{c}$. Putting in matrix form and using (45)–(46), we have

$$\mathbf{W}_o^H\mathbf{a}(z) = \{\bar{\mathbf{G}}^H\mathbf{a}_K(z)\}\{\mathbf{c}^H\mathbf{a}_L(z)\} \tag{48}$$

$$\mathbf{a}^T(z^{-1})\mathbf{W}_o = \{\mathbf{a}_K^T(z^{-1})\bar{\mathbf{G}}\}\{\mathbf{a}_L^T(z^{-1})\mathbf{c}\} \tag{49}$$

where

$$\bar{\mathbf{G}} = [\mathbf{g}_1|\mathbf{g}_2|\cdots|\mathbf{g}_K]. \tag{50}$$

Substitution of (48)–(49) in (34) leads to

$$\Phi(z) = \{\mathbf{a}_L^T(z^{-1})\mathbf{c}\mathbf{c}^H\mathbf{a}_L(z)\}\{\mathbf{a}_K^T(z^{-1})\bar{\mathbf{G}}\bar{\mathbf{E}}_B\mathbf{P}\bar{\mathbf{E}}_B^H\bar{\mathbf{G}}^H\mathbf{a}_K(z)\}. \tag{51}$$

An interesting point gleaned from (51) is that we have decomposed $\Phi(z)$ in two individual factors accounting for $\mathbf{c}$ and $\bar{\mathbf{G}}$, respectively. The factor involving $\mathbf{c}$ is known *a priori* and thus contains no information about the DOA's. As a result, the DOA estimates must be determined with the $2(K-1)$th order polynomial

$$\Phi_K(z) = \mathbf{a}_K^T(z^{-1})\bar{\mathbf{G}}\bar{\mathbf{E}}_B\mathbf{P}\bar{\mathbf{E}}_B^H\bar{\mathbf{G}}^H\mathbf{a}_K(z). \tag{52}$$

The structure in (52) suggests that we may regard it as the signal polynomial associated with a K-element LES array generated by the noise EV matrix $\bar{\mathbf{G}}\bar{\mathbf{E}}_B$. Thus, working with (52) instead of (34) leads to a substantial reduction in computational load if $K \ll M$.

B. Parallel Processing via Banded Transformation

Although the execution of polynomial rooting is greatly simplified with subarray beamforming, the procedure of choosing D signal roots out of the $2(K-1)$ roots of $\Phi_K(z)$ is still vague, especially at low SNR. Kumaresan [19] and Bresler [20] propose a scheme to convert the DOA estimation problem into that of rooting a Dth order polynomial and thus avoid the vagueness in determining the signal roots. They exploit the fact that the ideal noise subspace associated with an LES array is spanned by the columns of a banded Toeplitz matrix with bandwidth $D+1$. Motivated by their work, we conduct the following matrix conversion:

$$\bar{\mathbf{G}}\bar{\mathbf{E}}_B = \begin{bmatrix} \mathbf{b}_1 & & & 0 \\ & \mathbf{b}_2 & & \\ & & \ddots & \\ 0 & & & \mathbf{b}_{K-D} \end{bmatrix}\mathbf{T}_B \tag{53}$$

where $\mathbf{b}_l$, $l = 1,\ldots,K-D$ are $(D+1)\times 1$ vectors with a unit leading component, and $\mathbf{T}_B$ is a $(K-D)\times(K-D)$ nonsingular matrix. Note that the banded matrix in (53) has the same structure as that described in (39) and (42). Some algebraic manipulations yield

$$\mathbf{b}_l = \mathbf{M}(l : D+l, :)\mathbf{T}_B^{-1}(:, l) \quad l = 1,\ldots,K-D \tag{54}$$

and

$$\mathbf{T}_B^{-1}(:, l) = \begin{bmatrix} \mathbf{M}(1 : l, :) \\ \mathbf{M}(D+l+1 : K, :) \end{bmatrix}^{-1}\mathbf{e}_l \quad l = 1,\ldots,K-D \tag{55}$$

where

- $\mathbf{M}(n_1 : n_2, :)$ submatrix consisting of the n_1th to the n_2th row of $\bar{\mathbf{G}}\bar{\mathbf{E}}_B$
- $\mathbf{T}_B^{-1}(:, l)$ lth column of $\mathbf{T}_B^{-1}$
- $\mathbf{e}_l$ lth column of the $(K-D)\times(K-D)$ identity matrix.

Substitution of (53) back into (52) leads to

$$\Phi_K(z) = \mathbf{a}_{D+1}^T(z^{-1})\mathbf{F}\mathbf{D}(z^{-1})\mathbf{T}_B\mathbf{P}\mathbf{T}_B^H\mathbf{D}(z)\mathbf{F}^H\mathbf{a}_{D+1}(z) \tag{56}$$

where $\mathbf{a}_{D+1}(z) = \mathbf{a}(z)$ with $M = D+1$,

$$\mathbf{D}(z) = \text{Diag}\{1, z, \ldots, z^{K-D-1}\} \tag{57}$$

and

$$\mathbf{F} = [\mathbf{b}_1|\mathbf{b}_2|\cdots|\mathbf{b}_{K-D}]. \quad (58)$$

Note that except for the z-dependent term $\mathbf{D}(z)$, the polynomial in (56) is essentially that associated with a $(D+1)$-element LES array. To fully exploit this reduction in dimension, it is natural to replace $\mathbf{D}(z)$ with a constant matrix by fixing $z = z_o$:

$$\Phi_K(z|z_o) = \mathbf{a}_{D+1}^T(z^{-1})\mathbf{F}\mathbf{D}(z_o^{-1})\mathbf{T}_B\mathbf{P} \mathbf{T}_B^H\mathbf{D}(z_o)\mathbf{F}^H\mathbf{a}_{D+1}(z) \quad (59)$$

Comparing (59) and (56), we see that in order to achieve the performance of working with the original signal polynomial, we must choose $z_o \approx z_i = e^{j\tau f_o u_i}$ in estimating u_i. This dictates that a set of reduced-order signal polynomials $\Phi_K(z \mid \tilde{z}_i)$, $i = 1, \ldots, D$ be constructed with $\tilde{z}_i \approx z_i$, $i = 1, \ldots, D$. To determine $\hat{u}_i$, the corresponding signal root $\hat{z}_i$ is determined as a root of $\Phi_K(z \mid \tilde{z}_i)$ closest to $\tilde{z}_i$, that is, only a single DOA estimate is extracted from each reduced order polynomial.

The major difficulty of the above procedure is that it requires the knowledge of the DOA's we are trying to estimate. As a practical approach, we may decompose the effective spatial passband of the reference beamforming matrix into I_s disjoint sectors centered at $\bar{u}_m$, $m = 1, \ldots, I_s$, and construct

$$\Phi_K(z \mid \bar{z}_m) = \mathbf{a}_{D+1}^T(z^{-1})\mathbf{F}\mathbf{D}(\bar{z}_m^{-1})\mathbf{T}_B \mathbf{P}\mathbf{T}_B^H\mathbf{D}(\bar{z}_m)\mathbf{F}^H\mathbf{a}_{D+1}(z) \quad m = 1, \ldots, I_s \quad (60)$$

with $\bar{z}_m = e^{j\tau f_o \bar{u}_m}$, $m = 1, \ldots, I_s$. As long as the size of the sector is relatively small, we may approximate $\Phi_K(z)$ by $\Phi_K(z \mid \bar{z}_m)$ for the mth sector with high accuracy. By rooting (60) in parallel, we obtain totally I_s sets of roots $\hat{z}_{im}$ and $1/\hat{z}_{im}^*$, $i = 1, \ldots, D$, $m = 1, \ldots, I_s$. Since u_i should be best estimated with the polynomial associated with the sector containing u_i, we should pick those roots satisfying

$$\frac{1}{\tau f_o}\arg\{\hat{z}_{im}\} \in \text{ sector } m \quad i = 1, \ldots, D; m = 1, \ldots, I_s. \quad (61)$$

If the total number of roots picked exceeds D, then those D ones closest to the unit circle are selected. It should be pointed out that under no noise/error conditions are the I_s sets of roots identical since replacing (52) by (60) is in fact tantamount to replacing $\mathbf{P}$ by z-dependent positive semidefinite weighting matrices.

For practical noisy cases, the above developed parallelized DOA estimator is suboptimum since the modified z-dependent weighting matrices are no longer optimum even if $\mathbf{P}$ is so chosen. This results in degradation in estimation accuracy at low SNR. On the other hand, even with the true DOA's used as the fixing angles, $\bar{u}_m$, $m = 1, \ldots, I_s$, the DOA estimates will not be exactly identical to those obtained with the true signal polynomial. This is because that the signal roots associated with the true signal polynomial may not lie on the unit circle, but the conversion from (56) to (60) inherently assumes that all signal roots are on the unit circle. In some sense, the parallelized estimator behaves as a mixture of the root-form and spectral-form estimators. According to the argument of Rao and Hari [17], one can predict that the parallelized estimator should exhibit poorer resolution capability at low SNR than the full dimensional root-form estimators.

C. Further Simplification via Rank-One Approximation

We note that under no noise/error conditions is the banded matrix on the right-hand side of (53) also Toeplitz [20], i.e., $\mathbf{b}_1 = \mathbf{b}_2 = \cdots = \mathbf{b}_{K-D}$. It follows from (58) that under moderately good conditions, $\mathbf{F}$ is approximately rank one. This suggests that we may replace the matrices on the right-hand side of (60) by their rank-one representations:

$$\mathbf{F}\mathbf{D}(\bar{z}_m^{-1})\mathbf{T}_B\mathbf{P}\mathbf{T}_B^H\mathbf{D}(\bar{z}_m)\mathbf{F}^H \Rightarrow \mathbf{F}\mathbf{D}(\bar{z}_m^{-1})\mathbf{T}_B\mathbf{p}_m\mathbf{p}_m^H\mathbf{T}_B^H\mathbf{D}(\bar{z}_m)\mathbf{F}^H \quad m = 1, \ldots, I_s \quad (62)$$

where $\mathbf{p}_m$ is a $(K-D) \times 1$ vector. Note that we put the subscript m to emphasize the dependence on different sectors. For example, choosing $\mathbf{p}_m$ to be the transpose of the first row of $\mathbf{F}\mathbf{D}(\bar{z}_m^{-1})\mathbf{T}_B$ corresponds to Root-Minimum-Norm applied on a $(D+1)$-element LES array. With the structures of (62), we need only work with the set of Dth order polynomials:

$$\tilde{\Phi}_K(z \mid \bar{z}_m) = \mathbf{p}_m^H\mathbf{T}_B^H\mathbf{D}(\bar{z}_m)\mathbf{F}^H\mathbf{a}_{D+1}(z) \quad m = 1, \ldots, I_s. \quad (63)$$

In summary, except for the initial construction of beamforming matrices and the BI transformation, the above developed subarray-based DOA estimation procedure requires

1) performing a $K \times K$ generalized eigen-decomposition
2) solving in parallel $K-D$ systems of equations of size $K-D$
3) rooting in parallel I_s $2D$th (or Dth) order polynomials.

We thus conclude that significant saving in computations can be achieved, compared with the conventional Root-MUSIC algorithm for the case $D \approx K \ll M$.

D. Design of Subarray-Based Reference Beamforming Matrix

The factorization described in (47) does not hold for a particular desired beamforming matrix $\mathbf{W}_d$. One way to retain the merits of $\mathbf{W}_d$ using subarray beamforming is to judiciously choose $\mathbf{c}$ and $\mathbf{g}_k$, $k = 1, \ldots, K$ so that $\mathbf{W}_o$ is close to $\mathbf{W}_d$. Using again the LS fit technique leads to the following problem:

$$\min_{\mathbf{c},\mathbf{g}_1,\ldots,\mathbf{g}_K} ||\mathbf{W}_o - \mathbf{W}_d||_F^2 \equiv \min_{\mathbf{c},\mathbf{g}_1,\ldots,\mathbf{g}_K} \sum_{k=1}^{K} ||\mathbf{w}_{ok} - \mathbf{w}_{dk}||^2. \quad (64)$$

Invoking the structures in (47), we can rewrite (64) as

$$\min_{\mathbf{C},\bar{\mathbf{G}}} ||\mathbf{C}\bar{\mathbf{G}} - \mathbf{W}_d||_F^2 \equiv \min_{\mathbf{c},\tilde{\mathbf{G}}} ||\tilde{\mathbf{G}}\mathbf{c} - \tilde{\mathbf{w}}_d||^2 \quad (65)$$

where $\mathbf{C}$ and $\bar{\mathbf{G}}$ are given by (42) and (50), respectively:

$$\tilde{\mathbf{G}} = \begin{bmatrix} \mathbf{G}_1 \\ \mathbf{G}_2 \\ \vdots \\ \mathbf{G}_K \end{bmatrix} \quad (66)$$

and

$$\tilde{\mathbf{w}}_d = \begin{bmatrix} \mathbf{w}_{d1} \\ \mathbf{w}_{d2} \\ \vdots \\ \mathbf{w}_{dK} \end{bmatrix}. \quad (67)$$

Equation (65) has no closed-form solution in general. Instead of solving it with brute force, we suggest that the problem be decomposed into two individual stages for which in one stage, we solve for the common weight factor $\mathbf{c}$, whereas in the other, we solve for the uncommon weight factor $\mathbf{g}_k$, $k = 1, \ldots, K$. Assuming that an initial guess of $\mathbf{c}$ (or $\mathbf{C}$) is available and solving the left-hand side of (65) for $\bar{\mathbf{G}}$, we get

$$\bar{\mathbf{G}} = \left(\mathbf{C}^H\mathbf{C}\right)^{-1}\mathbf{C}^H\mathbf{W}_d. \quad (68)$$

Constructing $\tilde{\mathbf{G}}$ with the obtained $\bar{\mathbf{G}}$ in accordance with (39), (50), and (66) and solving the right-hand side of (65) for $\mathbf{c}$ yields

$$\mathbf{c} = \left(\tilde{\mathbf{G}}^H\tilde{\mathbf{G}}\right)^{-1}\tilde{\mathbf{G}}^H\tilde{\mathbf{w}}_d. \quad (69)$$

We may proceed to construct $\mathbf{C}$ and solve for a new $\bar{\mathbf{G}}$. The procedure is then alternately executed between (68) and (69) until the solutions converge.

V. Computer Simulations

Computer simulations are presented to ascertain the performance of the proposed BI-CSSM processing in a multiple wideband sources environment. The array employed was LES, consisting of $M = 15$ elements with a half-wavelength spacing at the center frequency f_c. The normalized bandwidth of the receiver was 40%. Signals from three wideband sources arrived at 8, 11, and 35° with respect to the broadside of the array. The angular separation between the first two sources was slightly less than half a 3-dB beamwidth of the array ($\approx 7.64°$). The received signals due to the three sources are assumed to be uncorrelated bandpass white Gaussian processes with the same spectral density height S_o. It should be pointed out that although we here consider only uncorrelated sources, the proposed method works for coherent case as well. Spatially white Gaussian bandpass noise with a spectral density height N_o, independent of the received signals, was present at each array element. The signal-to-noise ratio (SNR) in decibels per array element was defined as $10\log_{10}(S_o/N_o)$. A bandpass filter bank was used to decompose the receiving band into $J = 33$ uniformly distributed frequency bins so that the output data from each bin may be modeled as narrowband. For each execution of DOA estimation, $N = 30$ snapshots were collected at each of the 33 bins.

The first set of simulations compares the performance of BI-CSSM with that of regular CSSM. For all cases, the reference frequency was chosen as $f_o = f_1$. For BI processing, the set of $K = 7$ minimum focusing error weight vectors corresponding to Fig. 1 was used to constitute the reference beamforming matrix. The beamforming matrices for the remaining 32 frequencies were constructed in accordance with (21). The FOV was $[-1, 1]$ and the weighting function was the same as that given by (31). For CSSM, 33 focusing matrices were formed based on the dummy direction-vector constrained (DDVC) approach, with focusing angles $\{-30, -21, -12, -3, 6, 8, 11, 13, 23, 33, 35, 37, 46, 55, \text{ and } 64°\}$, and the rotational signal subspace (RSS) approach [7], with focusing angles $\{8, 11, \text{ and } 35°\}$. Note that we have assumed that the correct DOA's were used for the focusing angles in DDVC-CSSM and RSS-CSSM. The focused data snapshots were then transformed into beamspace using the same reference beamforming matrix as that used in BI-CSSM. The resulting sample root-mean-squared error (RMSE) of the DOA estimates obtained from 50 independent trials of the conventional beamspace MUSIC algorithm were shown in Fig. 4(a) for various SNR levels. Note that each RMSE value represents the average of the sample RMSE's for the three sources. Surprisingly, DDVC-CCSM did not outperform BI-CSSM, even though perfect focusing angles were used. A plausible reason for this is that the dummy direction vectors were not optimally chosen in DDVC-CSSM. BI-CSSM, on the other hand, does not suffer any performance degradation due to the imperfections in the preliminary processing. This is a demonstration of the reliability of the BI-CSSM preprocessing. As would be expected, RSS-CSSM performs best among the three methods, owing to the unitariness of the focusing matrices used, and because perfect focusing angles were used. Fig. 4(b) shows the probability of resolution versus SNR for the two sources from 8 and 11°. RSS-CSSM again outperforms the other two, with a resolution threshold of -5 dB. We observe that BI-CSSM performs slightly better than DDVC-CSSM, both exhibiting a resolution threshold of 0 dB. This is a demonstration of the efficacy of BI-CSSM in resolving closed-spaced sources.

Although RSS-CSSM exhibits excellent resolution capability and estimation accuracy compared with other CSS methods, its performance is affected greatly by the choosing of focusing angles. To demonstrate this effect, we repeated the above simulation work for RSS-CSSM but with a new set of focusing angles $\{7.6, 9.5, 11.4, 30.1, 32, \text{ and } 33.9°\}$. In this case, it was assumed that preliminary DOA estimation was performed. The source at 35° was not accurately detected, and consequently, focusing was only effective for the two closely spaced sources. The average sample RMSE of the DOA estimates obtained from 50 independent trials of the conventional beamspace MUSIC algorithm were shown in Fig. 5(a). Observing the results, we find that RSS-CSSM was not able to provide reliable DOA estimates at any SNR level. Interestingly, the sample RMSE did not decrease as the SNR was increased. This is in contrast with BI-CSSM, which apparently improved with higher SNR. The large sample RMSE associated with RSS-CSSM reflects the estimation bias due to the errors in the focusing angles. This is a drawback not shared by BI-CSSM. The probability of resolution versus SNR curves for the two sources from 8 and 11° were plotted in Fig. 5(b). We

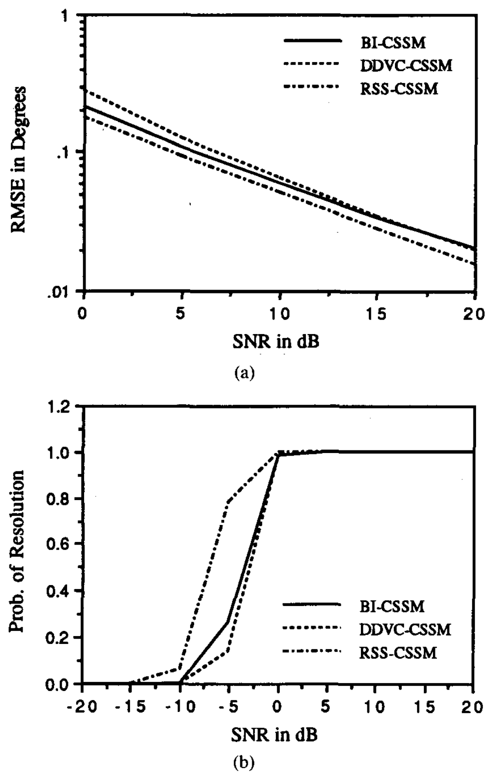

Fig. 4. Comparison of the performance of BI-CSSM, DDVC-CSSM, and RSS-CSSM for several SNR values: (a) Average sample RMSE's and (b) probability of resolution.

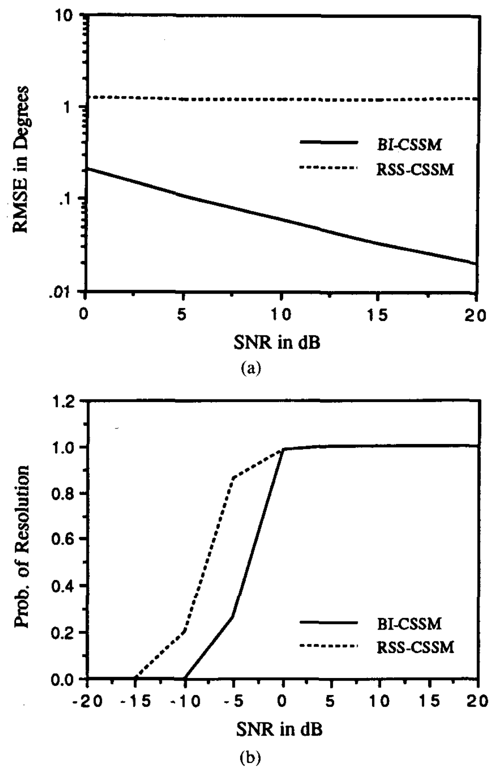

Fig. 5. Comparison of the performance of BI-CSSM and RSS-CSSM (with errors in focusing angles) for several SNR values: (a) Average sample RMSE's; (b) probability of resolution.

see that in spite of the large estimation bias, RSS-CSSM still exhibits a lower resolution threshold than BI-CSSM.

The third set of simulations was conducted to ascertain the effectiveness of the beamspace reduced-order Root-MUSIC (RORoot-MUSIC) procedure outlined in Sections IV-A–IV-D when used in conjunction with BI-CSSM. The subarray-based reference beamforming matrix was constructed in accordance with the procedure described in Section IV-D using the aforementioned minimum focusing error beamforming matrix as the desired one to fit. Fig. 6 shows the superposition of the resulting reference beam patterns. We have found that for this particular case, the algorithm converged in 20 iterations, with a suitably chosen initial guess of **c**. Comparing Figs. 1 and 6, we observe that the new patterns were fairly close to the original ones over the entire passband. We also note that the new patterns exhibit several out-of-band "common nulls" corresponding to the common factor **c**. For the rooting of (60), the spatial band $[-40, 40°]$ was divided into $I_s = 8$ sectors centered at $\theta = \pm 5, \pm 15, \pm 25$, and $\pm 35°$. The resulting average sample RMSE of the DOA estimates obtained from 50 independent trials were depicted in Fig. 7(a). For comparison, we also include the results obtained with the conventional beamspace Root-MUSIC algorithm working with the same reference beamforming matrix. We see that the two methods provide comparable results for most SNR levels. As expected, conventional Root-MUSIC performed better at low SNR. Finally, the probability of resolution curves shown in Fig. 7(b) indicate that both methods exhibit a resolution threshold of -5 dB. Root-MUSIC is superior in that the degradation in performance at low SNR is more gradual than that associated with RORoot-MUSIC. To compare the numerical complexity of the two methods, we recorded the number of floating-point operations required for each execution of the two DOA estimation procedures. Impressively, the computational load of RORoot-MUSIC ($\approx 8 \times 10^4$ flops/execution) is less than 5% that of Root-MUSIC ($\approx 1.7 \times 10^6$ flops/execution). It should be noted that the disparity between the two numbers will be even greater as the number of elements increases.

VI. Conclusion

The BI focusing scheme was developed as an efficient means of beamspace wideband source localization. It performs beamspace transformation and focusing at the same time by judiciously constructing a set of beamforming matrices so that the resulting beamspace DOA matrices are essentially the same for all frequencies. These beamforming matrices achieve nearly perfect focusing over a large angular region within the FOV of the array without knowing *a priori* the spatial distribution of the wideband sources. For LES arrays, a fast root-form eigen-based method was proposed, which requires only solving in parallel several small systems of equations and rooting in parallel several polynomials with the order equal to

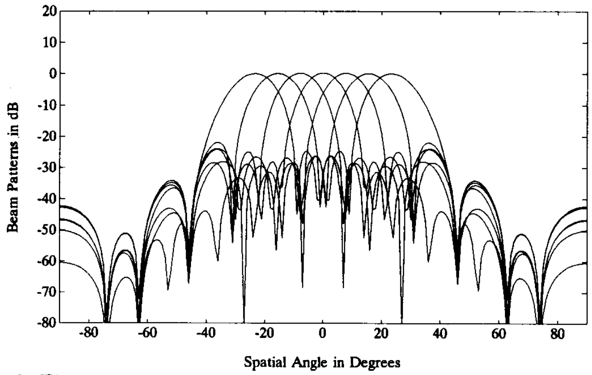

Fig. 6. Superposition of $K = 7$ subarray-formed beam patterns generated by an $M = 15$ element LES array.

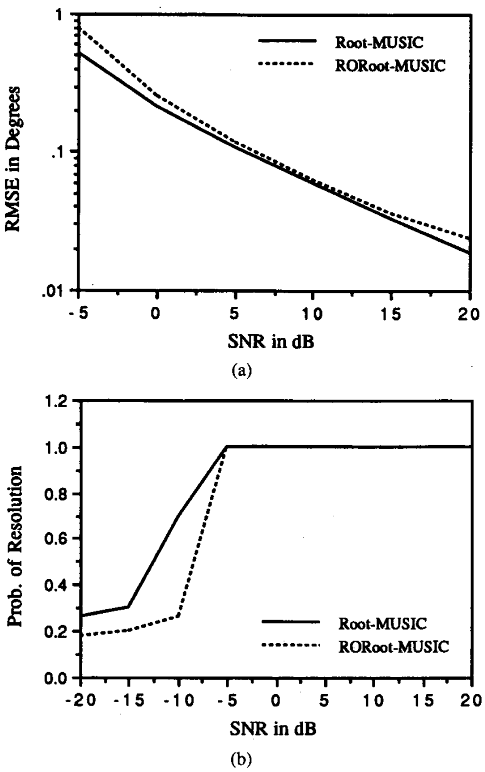

Fig. 7. Comparison of the performance of BI-CSSM working in conjunction with Root-MUSIC and reduced-order Root-MUSIC (RORoot-MUSIC) for several SNR values: (a) Average sample RMSE's; (b) probability of resolution.

the number of sources. Numerical examples show that the new method exhibits excellent estimation accuracy and is robust compared with the regular CSSM.

The proposed BI wideband beamforming scheme developed herein can be extended to a more complicated scenario involving strong out-of-band interference. In this case, the beamforming matrices $\mathbf{W}_j$, $j = 1, \ldots, J$ are constructed in such a fashion that each of the beam patterns exhibits a null in each of the interfering directions. To apply the fast root-form methods to a nonLES array, the BI transformation may be used as a means of both interpolation [18], [21] and focusing over a specified spatial band, that is, the DOA matrices associated with the J frequencies are transformed into the one associated with a virtual LES array operating at the reference frequency. The proposed method is suitable for real-time passive wideband source direction finding for which low computational complexity is critical. For example, in passive sonar applications, one may use an LES hydrophone array to localize a group of active underwater sources.

References

[1] G. Su and M. Morf, "Signal subspace approach for multiple wide-band emitter location," *IEEE Trans. Acoust. Speech Signal Processing*, vol. ASSP-31, pp. 1502–1522, Dec. 1983.

[2] H. Wang and M. Kaveh, "Coherent singal-subspace processing for the detection and estimation of angles of arrival of multiple wideband sources," *IEEE Trans. Acoust. Speech Signal Processing*, vol. ASSP-33, pp. 823–831, Aug. 1985.

[3] S. Nawab, F. Dowla and R. Lacoss, "Direction determination of wide-band signals," *IEEE Trans. Acoust. Speech Signal Processing*, vol. ASSP-33, pp. 1114–1122, Oct. 1985.

[4] A. K. Shaw and R. Kumaresan, "Estimation of angles of arrivals of broadband sources," in *Proc. ICASSP '87*, Apr. 1987, pp. 2296–2299.

[5] K. M. Buckley and X. L. Xu, "Reduced-dimension beam-space broadband source localization: Preprocessor design," *Advanced Algorithms Architectures Signal Processing*, vol. 975, pp. 368–376, 1988.

[6] K. M. Buckley and L. J. Griffiths, "Broad-band signal-subspace spatial-spectrum (BASS-ALE) estimation," *IEEE Trans. Acoust. Speech Signal Processing*, vol. 36, pp. 953–964, July 1988.

[7] H. Hung and M. Kaveh, "Focusing matrices for coherent signal-subspace processing," *IEEE Trans. Acoust. Speech Signal Processing*, vol. 36, pp. 1272–1281, Aug. 1988.

[8] G. Clergeot and O. Michel, "New simple implementation of the coherent signal-subspace method for wide band direction of arrival estimation," in *Proc. ICASSP ' 89*, 1989, pp. 2764–2767.

[9] J. Krolik and D. N. Swingler, "Multiple wideband source location using steered covariance matrices," *IEEE Trans. Acoust. Speech Signal Processing*, vol. 37, pp. 1481–1494, Oct. 1989.

[10] B. Ottersten and T. Kailath, "Direction-of-arrival estimation for wide-band signals using the ESPRIT algorithm," *IEEE Trans. Acoust. Speech Signal Processing*, vol. 38, pp. 317–327, Feb. 1990.

[11] J. Krolik and D. Swingler, "Focused wide-band array processing by spatial resampling," *IEEE Trans. Acoust. Speech Signal Processing*, vol. 38, pp. 356–360, Feb. 1990.

[12] A. J. Barabell, "Improving the resolution performance of eigenstructure based direction finding algorithms," in *Proc. ICASSP '83*, 1983, pp. 336–339.

[13] H. B. Lee and M. S. Wengrovitz, "Resolution threshold of beamspace MUSIC for two closely spaced emitters," *IEEE Trans. Acoust. Speech Signal Processing*, vol. 38, pp. 1545–1559, Sept. 1990.

[14] S. Anderson, "Optimum dimension reduction for sensor array signal processing," in *Conf. Rec. 25th Asilomar Conf. Signals Syst. Comput.*, Nov. 1991, pp. 918–922, vol. 2.

[15] P. Forster and G. Vezzosi, "Application of spheroidal sequences to array processing," in *Proc. ICASSP 87*, Apr. 1987, pp. 2267–2271.

[16] R. Kumaresan and D. W. Tufts, "Estimating the angles of arrival of multiple plane waves," *IEEE Trans. Aerospace Electron. Syst.*, vol. 19, pp. 134–138, Jan. 1983.

[17] B. Rao and K. Hari, "Performance analysis of root-MUSIC," *IEEE Trans. Acoust. Speech Signal Processing*, vol. 37, pp. 1939–1949, Dec. 1989.

[18] B. Friedlander and A. J. Weiss, "Direction finding for wide-band signals using an interpolated array," *IEEE Trans. Signal Processing*, vol. 41, pp. 1618–1635, Apr. 1993.

[19] R. Kumaresan and A. K. Shaw, "Superresolution by structured matrix approximation," *IEEE Trans. Antennas Propagat.*, vol. 36, pp. 34–44, Jan. 1988.

[20] Y. Bresler and A. Macovski, "Exact maximum likelihood parameter estimation of superimposed exponential signals in noise," *IEEE Trans. Acoust. Speech Signal Processing*, vol. 34, pp. 1081–1089, Oct. 1986.

[21] T. P. Bronez, "Sector interpolation of non-uniform arrays for efficient high resolution bearing estimation," in*Proc. ICASSP '88*, 1988, pp. 2885–2888.

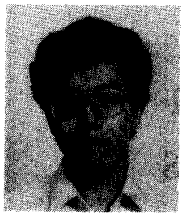

Ta-Sung Lee was born in Taipai, Taiwan, Republic of China, on October 20, 1960. He received the B.S. degree from National Taiwan University in 1983, the M.S. degree from the University of Wisconsin at Madison in 1987, and the Ph.D. degree from Purdue University in 1989, all in electrical engineering.

From 1987 to 1989, he was a David Ross Graduate Research Fellow at Purdue University. In the Spring of 1990, he joined the faculty of National Chiao Tung University, where he currently holds a position as associate professor in the Department of Communication Engineering. His present research interests include sensor array signal processing, adaptive antennas for mobile communications, underwater acoustic signal processing, and blind equalization.

Dr. Lee is a member of Phi Tau Phi.